Size Distribution of CO_2 Drops in a Static Mixer for Ocean Disposal

Hideo Tajima, Akihiro Yamasaki, and Fumio Kiyono
National Institute of Advanced Industrial Science and Technology (AIST), Tsukuba, Ibaraki 305-8569, Japan

Ho Teng
AVL Powertrain Engineering, Inc., Plymouth, MI 48170

DOI 10.1002/aic.10895
Published online May 8, 2006 in Wiley InterScience (www.interscience.wiley.com).

Keywords: CO_2, ocean disposal, drop size control, static mixer, hydrate

Introduction

Ocean sequestration of the anthropogenic CO_2 has been recognized as an effective measure for mitigating global warming.[1] Various methods for disposal of the CO_2 into the ocean have been proposed. These methods may be classified in three scenarios according to the depth at which CO_2 is disposed into the ocean: (1) disposal of CO_2 into shallow waters at a depth between 200 and 400 m below the ocean surface, under the pressure and temperature at which CO_2 is generally in the gas state[2]; (2) disposal of CO_2 into intermediate waters at a depth between 500 and 1500 m in the form of either liquid[3] or particles of hydrate[4]; and (3) disposal of CO_2 into deep waters at a depth $>$ 3000 m, where liquid CO_2 becomes denser than seawater and thus would descend to the seafloor, where it would form a storage pool.[5] To date, only the second scenario has been studied intensively as a result of having a benign environmental impact and less cost for implementation.

Because CO_2 is only slightly miscible in seawater, the CO_2–seawater system is unstable hydrodynamically and the liquid CO_2 injected into seawater breaks up into drops. Under the pressure (p) and temperature (T) of seawater at intermediate depths, liquid CO_2 is less dense than seawater; thus, the CO_2 drops—resulting from the ocean disposal—ascend toward the ocean surface, during which they would fully dissolve in seawater if their initial sizes are not too large. If p and T of seawater at the disposal site also satisfy those for formation of CO_2 hydrate (that is, $p > 44.5$ bar, $T < 283$ K), then a hydrate film could form on the CO_2 drops. Laboratory simulations demonstrated that the hydrate film formed on a CO_2 drop could significantly reduce its rate of dissolution in the ocean.[6,7] The environmental impact from the ocean disposal of CO_2 is determined by the level of increase in the CO_2 concentration in the local seawater induced by the CO_2 dissolution. To minimize the environmental impact, the initial sizes of the CO_2 drops and their distribution in the release as well as their dissolution distances (that is, the traveling distance before the drops fully dissolve in seawater) should be controllable parameters in the design of a CO_2 disposal process; thus, Brewer et al.[8] estimated the relation between the traveling distance of CO_2 drop and the drop diameter with only one drop. However, because real CO_2 injection has the drop size distribution, then it is necessary to complete an overall estimation and control for injection of CO_2 drops covered with hydrate.

In a previous article,[9] the authors of this work proposed to use a static mixer as a device to control the initial sizes of the CO_2 drops and their distribution in the release, and this proposed concept was validated by a laboratory-scale experiment under a simulated condition for seawater at intermediate depths. The experiment demonstrated that CO_2 drops could be produced continuously by the static mixer and the averaged size of the drops and their number density in the release could be controlled by governing the flows of seawater and liquid CO_2. In the aforementioned work, the investigation was focused on the postmixing parameters, that is, the drop sizes and their distribution in the release from the static mixer. Because the mixer was made of stainless steel, it was not possible to study the drop formation process and the variation in drop sizes along the mixer. A proper design of a static mixer, which can produce a desirable size distribution of the CO_2 drops, requires full understanding of the relationship between the number of mixing elements and the drop sizes and their distribution. To that end, the objective of this article is to investigate the drop

Correspondence concerning this article should be addressed to A. Tajima at hideo-tajima@aist.go.jp.

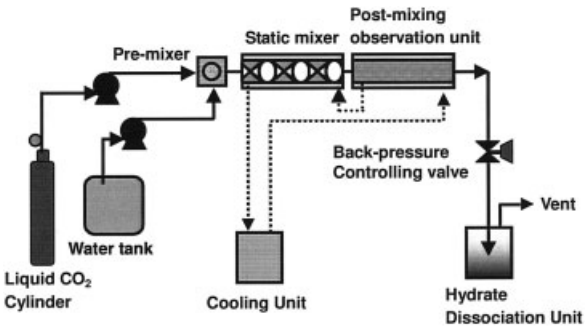

Figure 1. Experimental system.

formation process and the effect of the number of mixing elements in the mixer on the drop sizes and their distribution.

Experimental System

Figure 1 shows the experimental system for this investigation. Major components of the experimental system were a premixing unit, a static mixer, and a postmixing observation section. The premixing unit was a stainless steel block with a cubic cavity with its two inlet ports connected respectively to the supply lines of liquid CO_2 and water and with its outlet port connected to the inlet of the static mixer. Figure 2 shows the structure of the Kenics-type static mixer, designed particularly for this investigation. The tube of the static mixer, 300 mm in length, 10.6 mm in inner diameter, made from Pyrex® glass (which is chemically inert with CO_2), could stand a maximum pressure of 2.0 MPa. To increase the system pressure, the Pyrex® glass tube was inserted into a larger polycarbonate tube (noting that polycarbonate is not fully chemically compatible with CO_2), which could stand a maximum pressure of 15 MPa. The annular space between the two tubes was filled with water the pressure of which could be adjusted in balance with that inside the Pyrex® glass tube by a piston-type pressure equalizer (Nitto Koatsu Co., Tokyo, Japan). In this way, the maximum system pressure was increased to 15 MPa, equivalent to the static pressure of seawater at the depth of 1500 m. The outside of the composite tube of the static mixer was an acryl tube, the housing of which (the annular space between the polycarbonate and acryl tubes) formed a water jacket for the static mixer. The cooling water from a thermal bath was circulated through the water jacket. The Kenics inserts or mixing elements (SUS 316; Noritake Co., Ltd., Nagoya, Japan) had a length-to-diameter ratio of 1.5. The basic unit of the static mixer consisted of six mixing elements, although the mixer could also be extended with more mixing elements, achieved by interconnection of several basic units as shown in Figure 2. The postmixing observation section was the same as that used in the previous investigation, the structure and dimensions of which were previously detailed.[9]

In experiments, liquid CO_2 from a CO_2 cylinder and precooled water from a water tank were introduced into the system through the premixing unit, where the two fluids merged and were then charged to the static mixer. Before being introduced into the system, both fluids were pressurized by pumps. The system pressure was controlled with an accuracy of ± 0.01 MPa by a pressure regulator installed downstream of the observation section. The system temperature was controlled by the cooling water circulated in a loop formed by the thermal bath and water jackets of the static mixer and the observation section, with an accuracy of ± 0.1 K. Because both the static mixer and the observation section were transparent, the drop formation process in the mixer and the release from the mixer could be observed and recorded by a high-speed video camera (VFC-1000; FOR-A Corp. of America, New York, NY). Snapshots of the transient mixing process also were taken and the digitalized images then analyzed with a Power Macintosh G4 computer using an image analysis program (Image J-1.27, developed by the National Institutes of Health, Bethesda, MD). The drop sizes and their distribution were analyzed statistically and a typical sample contained 700–900 drops selected randomly.

Results and Discussion

Figure 3 shows a snapshot of the formation process of liquid CO_2 drops in water in a static mixer at each mixing element. The temperature was 277 K and the pressure was 7.0 MPa, conditions that correspond to the ocean depth at 700 m, and liquid CO_2 drops always were covered with a thin hydrate film. Flow velocity of the water phase was 9.5 cm/s and that of liquid CO_2 was 0.83 cm/s. The Reynolds number (Re) was 919 on the basis of the mixer diameter, indicating a laminar flow region. Relatively large and irregularly shaped CO_2 drops formed at the premixing unit were divided, rotated, and mixed after entering the mixing elements. The drop size was reduced and the shape of the drops became more spherical as they passed through the static mixer. The size distribution of the liquid CO_2 drops observed at each mixing element is shown in Figure 4. The drop size distribution was obtained by analyzing the captured images of 700–900 drops observed in between two mixing elements. The mixing elements were numbered from the upstream side of the mixer. At the location between the elements of Nos. 7 and 8, the drop size distributed in the range of 0.2 to 1.8 mm and multiple peaks were observed. As the fluid proceeded through the mixer, the distribution peaks at the larger size region (>1 mm) were reduced and the peak at the smallest drop size region increased. Thus, the broader distribution with multiple peaks at the earlier stage of the

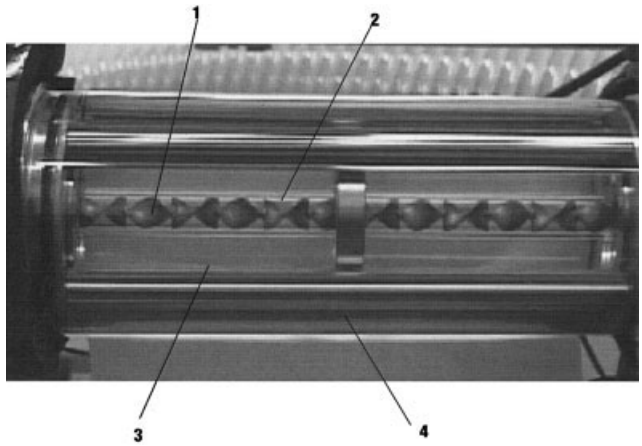

Figure 2. Structure of the static mixer used in this study.

1: Kenics-type mixing elements; 2: Pyrex® glass tube; 3: polycarbonate tube; 4: acryl tube (water jacket).

Figure 3. Development of CO_2 drops and their distribution in water in the static mixer.

mixing shifted to a sharper distribution with the sharper peak located at the smaller size region.

Such a variation of the drop size distribution of liquid CO_2 was also observed under conditions with higher water-phase velocities, and the transition of the size distribution was more prominent for these cases as shown in Figures 5 and 6. Figure 5 shows the variation of the size distribution in the static mixer under conditions where the CO_2 flow velocity was 0.83 cm/s, the water-phase velocity was 30.2 cm/s, and Re = 3065, of which the Reynolds number shows the transition region from laminar to turbulent. The size distribution observed at the first two elements (Nos. 1 and 2) was much broader than that observed after the 5th element. After the 5th element, the size distribution gradually changed as the liquid CO_2 drops proceeded through the mixer, and finally a sharp, Gaussian-shaped distribution curve was observed at the 11th and 12th elements. A similar type of variation was observed for the condition with higher water-phase velocity (56.7 cm/s, Re = 5807, turbulent region) as shown in Figure 6. However, the shape of the size distribution observed at the 9th and 10th elements was sharper than that for the case with lower phase velocity as shown in Figures 4 and 5. The influence of the water-phase velocity on the size distribution is shown in Figure 7, where the size distributions observed between the 9th and 10th elements were presented for various water-phase velocities. A sharp Gaussian-like distribution was observed for the highest water flow velocity at 56.7 cm/s, corresponding to a turbulent condition (Re = 5807), whereas a broader distribution was observed for the laminar flow condition where the phase velocity of water is as low as 9.5 cm/s (Re = 919). For transition flow conditions, where the phase velocity of water is 30.2 cm/s (Re = 3065), the size distribution is close to Gaussian, but broader than that observed under turbulent conditions. Thus, the drop size of liquid CO_2 in water in the static mixer is influenced by the number of mixing elements and water flow velocity.

The shift of the drop size distribution can be represented by the average size and the standard deviation of the drop size. For this purpose, the Sauter mean diameter (SMD) used in this study is defined as

$$SMD = \frac{\sum N_i D_i^3}{\sum N_i D_i^2} \tag{1}$$

where N_i is the number of CO_2 drops for the ith group having a diameter D_i. For each mixing element, the corresponding SMD for the CO_2 drops was calculated by Eq. 1. Variation in the SMD with the number of mixing elements is shown in Figure 8, where the temperature and pressure of the mixture and the phase velocities are the same as those of Figures 4–6. For the cases shown in Figure 8, the static mixer was extended and the number of mixing elements was increased to 24. It is

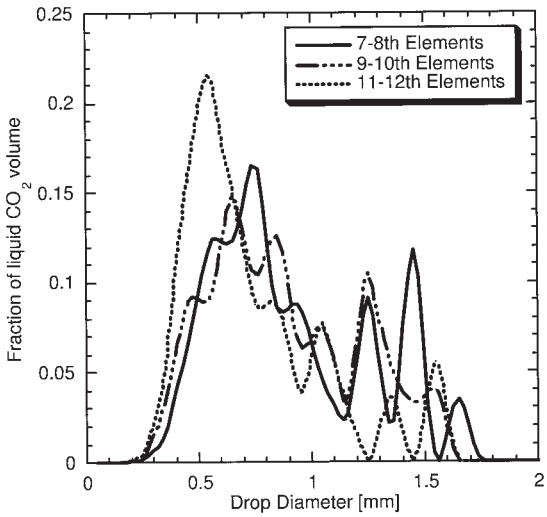

Figure 4. Drop size distribution of liquid CO_2 at the mixing elements in a Kenics-type static mixer under laminar flow region (Re = 919).

The drop size was observed at the location in between two mixing elements, which were numbered from the upstream side of the mixer. Mixture conditions: temperature (T) = 277 K; pressure (p) = 7.0 MPa; water flow velocity (V_{water}) = 9.5 cm/s; liquid CO_2 flow velocity (V_{CO_2}) = 0.83 cm/s.

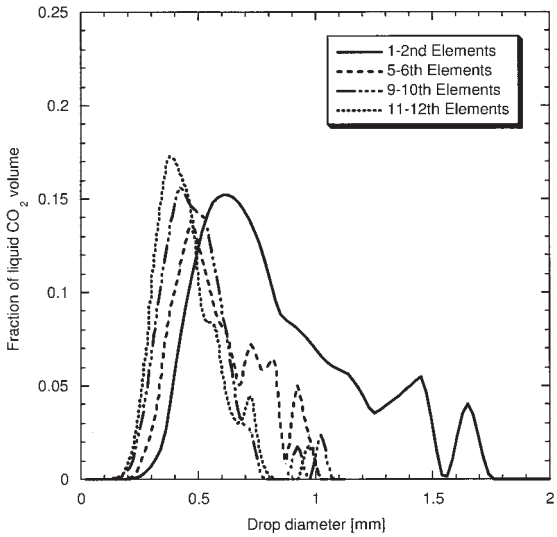

Figure 5. Drop size distribution of liquid CO_2 at the mixing elements in a Kenics-type static mixer under transition flow region (Re = 3065).

The drop size was observed at the location in between two mixing elements, which were numbered from the upstream side of the mixer. Mixture conditions: T = 277 K; p = 7.0 MPa; V_{water} = 30.2 cm/s; V_{CO_2} = 0.83 cm/s.

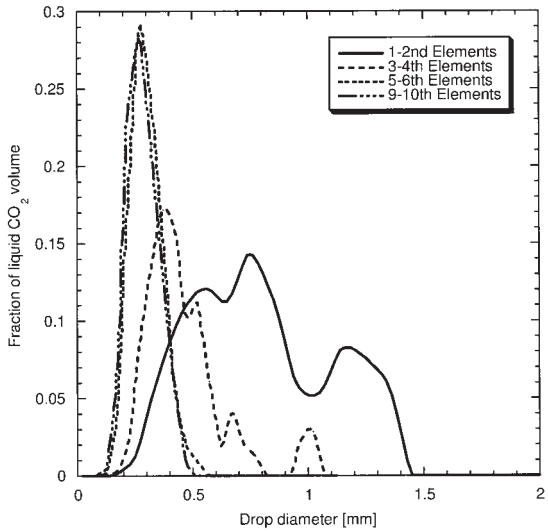

Figure 6. Drop size distribution of liquid CO_2 at the mixing elements in a Kenics-type static mixer under turbulent flow region (Re = 5807).

The drop size was observed at the location in between two mixing elements, which were numbered from the upstream side of the mixer. Mixture conditions: T = 277 K; p = 7.0 MPa; V_{water} = 56.7 cm/s; V_{CO_2} = 0.83 cm/s.

seen in each case of Figure 8 that, for the current experimental system, variation in the SMD for the CO_2 drops in the mixer has two stages: the first stage takes place primarily in the first five mixing elements, where the SMD decreases rapidly in an exponential pattern; the second stage is in the remaining mixing elements, where the SMD decreases linearly, having a small slope with increasing number of mixing elements: this indicates that the CO_2 drops underwent a significant size

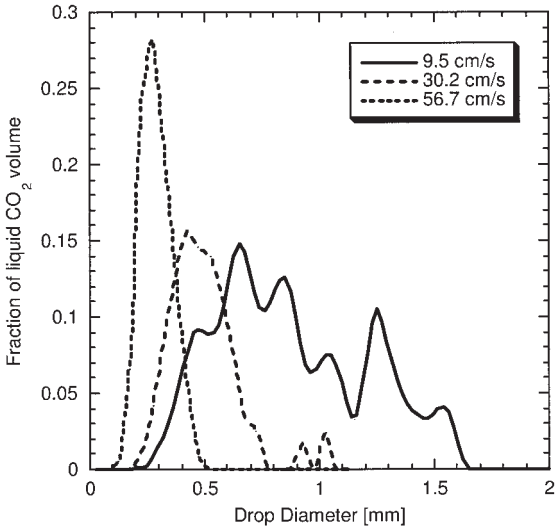

Figure 7. Influence of the water phase velocity on the liquid CO_2 drop size distribution observed at the location between 9th and 10th mixing elements.

Mixture conditions: T = 277 K; p = 7.0 MPa. Phase velocity of liquid CO_2 was fixed at 0.83 cm/s.

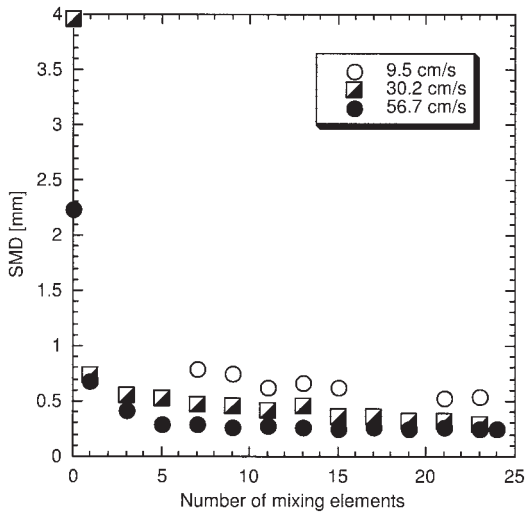

Figure 8. Variation of Sauter mean diameter (SMD) for CO_2 drops with the number of mixing elements in the static mixer.

Mixture conditions: T = 277 K, p = 7.0 MPa; V_{CO_2} = 0.83 cm/s; V_{water} = 9.5, 30.2, 56.7 cm/s.

change only in the first few mixing elements. It is apparent in Figure 8 that an increase in the continuous-phase velocity causes a decrease in both the SMD for the initial drops and that for the drops at the later mixing stage; and for the case of high Reynolds number (Re = 5807), especially, a further decrease in the SMD becomes negligibly small when the number of mixing elements is >10, as if the SMD is approaching an asymptotic value for the given system.

The dependency of the SMD on the continuous-phase velocity was previously reported by the present authors on the basis of the experimental results for a 12-element static mixer,[9] which can be given in dimensionless form as

$$\frac{SMD}{D_0} = 0.29 \times \mathrm{We}^{-0.48} \tag{2}$$

where D_0 is the inner diameter of the mixer; $\mathrm{We} = \rho u^2 D_0/\sigma_s$ is the Weber number on the basis of the continuous phase; ρ and u are, respectively, the density and the phase velocity for the continuous phase; and σ_s is the water-side surface tension. Note that if hydrate is formed at the CO_2–water interface, the surface tension from the CO_2 side may differ from that from the water side. Because Eq. 2 was derived on the basis of the drops released from a 12-mixing-element static mixer, it is reasonable to assume that it describes the cases where the CO_2 drops become fully dispersed and fairly uniformly distributed in water.

Recall that the right-hand side of Eq. 2 reflects the ratio of the disruptive energy on the drops (which tends to destabilize the drops) to the surface energy of the drops (which tends to stabilize the drops), at a given level of turbulence in the continuous phase. The turbulent intensity to which the drops are subjected increases in each next mixing element, that is, it is enhanced continuously along the mixer. Thus, a shortcoming of Eq. 2 is that it does not include information with respect to the degree of mixing in the mixer on the SMD for the drops

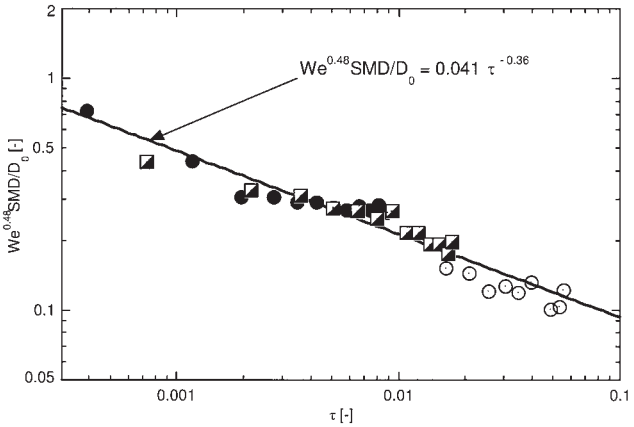

Figure 9. Relationship between the nondimensional number (SMD/D_0) × $We^{0.48}$ with nondimensional residence time τ.

released from the mixer. For a given static mixer, the degree of mixing is associated with the number of mixing elements involved in the mixing process[10,11]; moreover, it may also be estimated by the residence time for the mixture in the mixer.[12,13] Because our experimental results indicate the dependency of drop size on the number of mixing elements and continuous-phase flow velocity, the SMD for the CO_2 drops released from the static mixer may be expressed in a general form as

$$\frac{SMD}{D_0} = A \times \mathrm{We}^a \times \tau^b \tag{3}$$

where $a = -0.48$ and A and b are constants to be determined; $\tau = t_R/t^*$, $t_R = N_E L_E/u$ is the residence time, N_E is the number of mixing elements, and L_E is the length of an individual mixing element; $t^* = D_0^2/\nu_{CO_2}$ is a characteristic time, and ν_{CO_2} is the kinematic viscosity of CO_2 at the experimental temperature. Equation 3 may be rearranged in logarithmic form as

$$\log\left(\frac{SMD}{D_0}\mathrm{We}^{-a}\right) = \log(A) + b \times \log(\tau) \tag{4}$$

Equation 4 is a relationship between $(SMD/D_0) \times \mathrm{We}^{-a}$ and τ, which represents a straight line with $\log(A)$ and b being the intersect and the slope, respectively. The relationship between $(SMD/D_0) \times \mathrm{We}^{-a}$ and τ for the data presented in Figure 8 is plotted in Figure 9. All the SMD data points for various phase flow velocities of water can be correlated with a single line as shown in Figure 9. In other words, the SMD observed under a wide range of Reynolds numbers (laminar, transition, to turbulent conditions) can be correlated with a single correlation equation (Eq. 4), irrespective of the flow velocities. From the slope of the regression line, the parameters in Eq. 4 were determined as follows: $A = 0.041$ and $b = -0.36$; then Eq. 3 becomes

$$\frac{SMD}{D_0} = 0.041 \times \mathrm{We}^{-0.48} \times \tau^{-0.36} \tag{5}$$

It was previously found[9] that the sizes of the disperse CO_2 drops in water in the static mixer can be characterized by Gaussian distribution with respect to the SMD. Thus, departure of the drop sizes from the SMD may be analyzed by the standard deviation, which is given as

$$\sigma = \sqrt{\frac{\sum_{i=1}^{N}(D_i - SMD)^2}{N-1}} = SMD \times \sqrt{\frac{\sum_{i=1}^{N}(D_i/SMD - 1)^2}{N-1}} \tag{6}$$

where D_i is the diameter for the ith group of CO_2 drops and N is the total number of the drops in a sample. Equation 6 may be expressed in nondimensional form as

$$RSD = \sigma/SMD = \sqrt{\frac{\sum_{i=1}^{N}(D_i/SMD - 1)^2}{N-1}} \tag{7}$$

where RSD is a relative (or reduced) standard deviation. Relative standard deviations for the data in Figure 8 are presented in Figure 10. The RSD for the CO_2 drops decreases with the increasing number of mixing elements, and similar values of the RSD for transition and turbulent flow region cases are observed and values of the RSD for turbulent flow region are smaller than those for transition region at any number of mixing elements. It is seen in Figure 10 that values of the slope of curve for each case are very similar. Decay of the RSD with respect to the number of mixing elements N_E is found to follow an exponential relationship as

$$RSD = B \times \exp(-0.012 N_E) \tag{8}$$

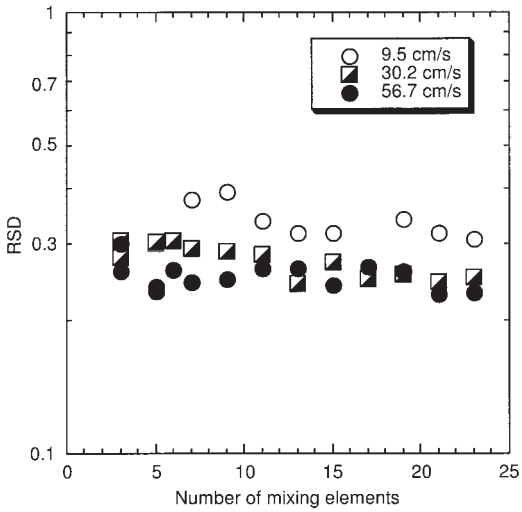

Figure 10. Variation of RSD for CO_2 drops with the number of mixing elements in the static mixer.

Mixture conditions: $T = 277$ K; $p = 7.0$ MPa; $V_{CO_2} = 0.83$ cm/s; $V_{water} = 9.5, 30.2, 56.7$ cm/s.

where B is a constant representing the value of RSD at the limiting condition $N_E = 0$. In Figure 10, the value of B is 0.4 for the laminar flow region and 0.31 for the transition and turbulent flow regions. Similar RSD–N_E relationships for different types of static mixers were reported in the literature.[10,14-16] This may reflect a common feature in static mixers, that is, the distribution of drop sizes is associated with the degree of mixing and, thus, with the number of mixing elements involved in the mixing process.

Conclusions

Variations in sizes and distributions of the CO_2 drops in the mixer were investigated visually and the corresponding data were analyzed using a statistical method. Liquid CO_2 entering the mixer underwent a continuous process of breakup and redistribution in the mixer, during which the initially large, irregular drops became small, spherical drops that fully dispersed in water. The first five mixing elements dominated the mixing and drop formation processes, and in the rest of the mixing elements the drop sizes varied to only a limited extent; after the first few mixing elements, the dispersed drops could be characterized by a Gaussian distribution with respect to the SMD. Departure of the drop sizes from the SMD was analyzed and the nondimensional standard deviation was found to decay exponentially with the number of mixing elements in the mixer. The nondimensional SMD was found to correlate well with the Weber number and the residence time for the CO_2 drops in the mixer, and the correlation obtained in this study would be useful in an optimum design of the static mixer for the ocean disposal of CO_2.

Literature Cited

1. Halmann MM, Steinberg M. *Greenhouse Gas Carbon Dioxide Mitigation*. Boca Raton, FL: Lewis Publishers; 1999.
2. Haugan PM, Drange H. Sequestration of CO_2 in the deep ocean by shallow injection. *Nature.* 1992;357:318-320.
3. Herzog HJ, Drake EM, Adams EE. CO_2 capture, reuse and storage technologies for mitigating global climate change—A white paper. DOE Report No. E-AF22-96PC01257. Washington, DC: Department of Energy; 1997.
4. Yamasaki A, Wakatsuki M, Teng H, Yanagisawa Y, Yamada K. A new ocean disposal scenario for anthropogenic CO_2: CO_2 hydrate formation in a submerged crystallizer and its disposal. *Energy.* 2000; 25:85-96.
5. Shindo Y, Fujioka Y, Ozaki M, Takeuchi K, Komiyama H. New concept of deep sea CO_2 sequestration. Proceedings of the International Symposium on CO_2 Fixation and Efficient Utilization of Energy; 1993:307-314.
6. Aya I, Yamase K, Yamada N. Stability of clathrate-hydrate of carbon dioxide in highly pressured water. *ASME HTD.* 1992;125:17-22.
7. Teng H, Yamasaki A, Shindo Y. The fate of CO_2 hydrate released in the ocean. *Int J Energy Res.* 1999;23:295-302.
8. Brewer PG, Peltzer ET, Friederich G, Rehder G. Experimental determination of the fate of rising CO_2 droplets in seawater. *Environ Sci Technol.* 2002;36:5441-5446.
9. Tajima H, Yamasaki A, Kiyono F, Teng H. New method for ocean disposal of CO_2 by a submerged Kenics-type static mixer. *AIChE J.* 2004;50:871-878.
10. Godfey JC. Static mixers. In: Harnby H, Edwards MF, Nienow AW, eds. *Mixing in the Process Industries*. 2nd Edition. Oxford, UK: Butterworth; 1992:225-249.
11. Paul EL, Atiemo-Obeng VA, Kresta SM. *Handbook of Industrial Mixing: Science and Practice*. Hoboken, NJ: Wiley–Interscience; 2004.
12. Konno M, Kosaka N, Saito S. Correlation of transient drop size in breakup process in liquid–liquid agitation. *J Chem Eng Jpn.* 1993;26: 37-40.
13. Nauman EB. On residence time and trajectory calculations in motionless mixers. *Chem Eng J.* 1991;47:141-148.
14. Hobbs DM, Muzzio FJ. Effects of injection location, flow ratio, and geometry on Kenics mixer performance. *AIChE J.* 1997;43:3121-3132.
15. Hobbs DM, Muzzio FJ. The Kenics static mixer: A three-dimensional chaotic flow. *Chem Eng J.* 1997;67:153-166.
16. Pahi MH, Muschelknautz E. Static mixers and their applications. *Int Chem Eng.* 1982;22:197-205.

Manuscript received Nov. 8, 2005, and revision received Apr. 10, 2006.